ChemPubSoc Europe

DOI: 10.1002/chem.201502799

CHEMISTRY
A European Journal
Full Paper

Imaging Agents

New Dual Fluorescent Probe for Simultaneous Biothiol and Phosphate Bioimaging

Sandra Resa,[a] Angel Orte,[b] Delia Miguel,[a] Jose M. Paredes,[b] Virginia Puente-Muñoz,[b] Rafael Salto,[c] Maria D. Giron,[c] Maria J. Ruedas-Rama,[b] Juan M. Cuerva,*[a] Jose M. Alvarez-Pez,[b] and Luis Crovetto*[b]

Dedicated to the memory of Professor Carlos Orte

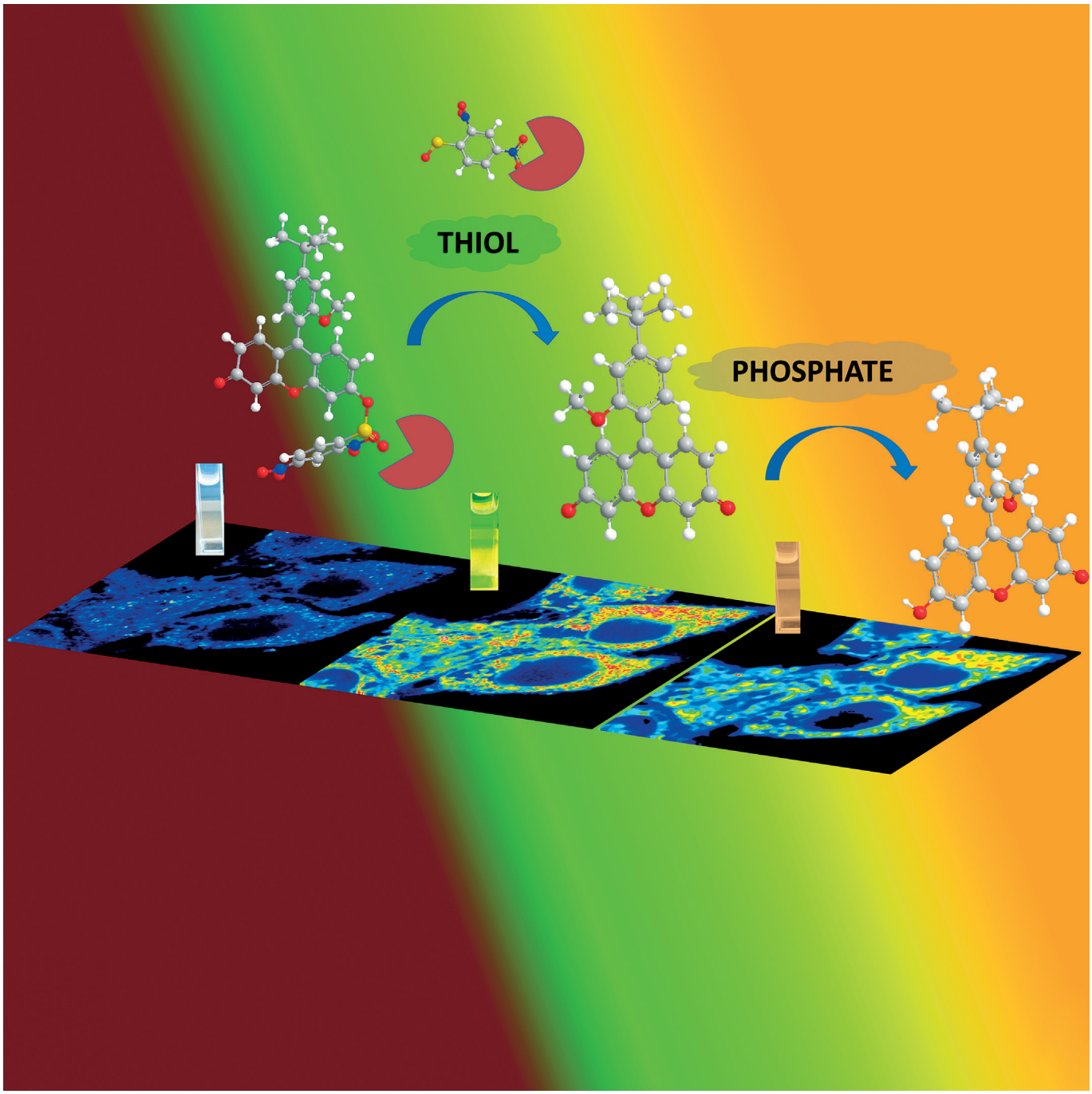

Abstract: The simultaneous detection of relevant metabolites in living organisms by using one molecule introduces an approach to understanding the relationships between these metabolites in healthy and deregulated cells. Fluorescent probes of low toxicity are remarkable tools for this type of analysis of biological systems in vivo. As a proof of concept, different naturally occurring compounds, such as biothiols and phosphate anions, were the focus for this work. The 2,4-dinitrobenzenesulfinate (DNBS) derivative of 9-[1-(4-*tert*-butyl-2-methoxyphenyl)]-6-hydroxy-3*H*-xanthen-3-one (Granada Green; GG) were designed and synthesized. This new sulfinyl xanthene derivative can act as a dual sensor for the aforementioned analytes simultaneously. The mechanism of action of this derivative implies thiolysis of the sulfinyl group of the weakly fluorescent DNBS-GG by biological thiols at near-neutral pH values, thus releasing the fluorescent GG moiety, which simultaneously responds to phosphate anions through its fluorescence-decay time. The new dual probe was tested in solution by using steady-state and time-resolved fluorescence and intracellularly by using fluorescence-lifetime imaging microscopy (FLIM) in human epithelioid cervix carcinoma (HeLa) cells.

Introduction

Fluorescent probes of low toxicity for multiplex sensing are remarkable tools for the analysis of biological systems.[1] To this end, different properties of the sensor must be related to unrelated bioanalytes, which is a difficult task. Within this context, we focused on very different naturally occurring compounds, such as biothiols and phosphate anions. Both of these compounds are widely present in living organisms and are relevant because their deregulation is related to cellular dysfunction. Biological thiols play crucial roles in biological systems; therefore, there has been a great effort to develop new methods to detect them over the last two decades. Among the methods for the detection and quantification of biological thiols, fluorescence approaches have proved to be the most suitable due to the advantages derived from their high sensitivity, simplicity, and low cost.[2] Phosphate ions play important roles in signal transduction and energy storage in biological systems; therefore, the detection and quantification of these ions inside the cell and extracellular media are relevant parameters in biological studies.[3] The measurement of intracellular phosphate ions as a marker of osteoblast differentiation and bone deposition combined with the assay of biothiol levels as a marker of oxidative stress would be a useful tool to address pathological processes that combine alterations of bone metabolism with increased oxidative stress, such as obesity and diabetes.[4]

To our knowledge, no fluorescent probes with the ability to measure these parameters simultaneously have been described to date. Therefore, we believe that a fluorescence-based multiplexed probe that can jointly sense biological thiols and inorganic phosphate ions inside and outside the cell would be of broad interest and utility.

The key point in this study was the careful selection of the fluorophore. In recent years, fluorescein-based compounds have evolved to yield simple structures that can retain their striking photophysical properties. Thus, for example, some aryl-[5] and alkyl-substituted xanthenones[6] have simplified the original prototropic equilibrium in fluorescein, thereby improving the analysis of the photophysical data (Figure 1). Therefore, these molecules have been used as fluorescent probes for many biologically relevant analytes, such as β-galactosidase,[5,7] hydrogen peroxide,[8] nucleotide pyrophosphatases/phosphodiesterases,[9] uridine diphosphate glucuronosyltransferase (UDPGT),[10] and BlaC hydrolase of *Mycobacterium tuberculosis*[11] as well as in Western blot analysis.[12] Within this context, a new methodology based on the dependence of the fluorescence-decay time of these xanthene-based dyes on the phosphate-buffer concentration at near physiological pH values has recently been developed in our laboratories.[13] The highest sensitivity was obtained with a customized compound, called Granada Green (GG), with a fine-tuned pK_a value of 7.3.[14]

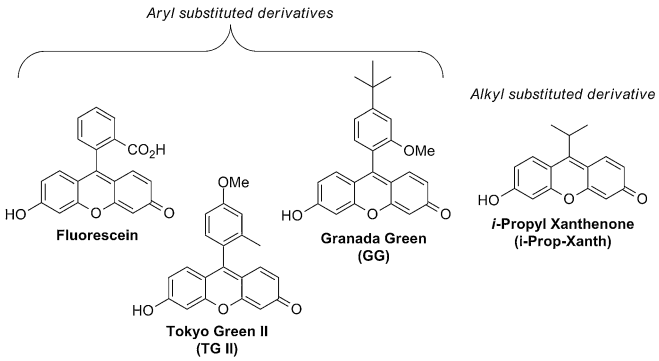

Figure 1. Xanthenone-based fluorescent compounds.

[a] *S. Resa, Dr. D. Miguel, Dr. J. M. Cuerva*
Department of Organic Chemistry
Faculty of Sciences, University of Granada
C. U. Fuentenueva s/n, 18071 Granada (Spain)
Fax: (+34) 958248437
E-mail: jmcuerva@ugr.es

[b] *Dr. A. Orte, Dr. J. M. Paredes, V. Puente-Muñoz, Dr. M. J. Ruedas-Rama, Prof. J. M. Alvarez-Pez, Dr. L. Crovetto*
Department of Physical Chemistry
Faculty of Pharmacy, University of Granada
Cartuja Campus, 18071 Granada (Spain)
Fax: (+34) 958244090
E-mail: luiscrovetto@ugr.es

[c] *Dr. R. Salto, Dr. M. D. Giron*
Department of Biochemistry and Molecular Biology
Faculty of Pharmacy, University of Granada
Cartuja Campus, 18071 Granada (Spain)

Supporting information and ORCID(s) from the author(s) for this article is available on the WWW under http://dx.doi.org/10.1002/chem.201502799.

Considering the remarkable properties of these compounds, we decided to demonstrate their selective ON–OFF fluorogenic behavior toward biological thiols. In this manner, the liberated fluorophore could be used for dual purposes: 1) for the detection of the presence of biothiols and 2) for providing information on the local phosphate-ion concentration (Scheme 1).

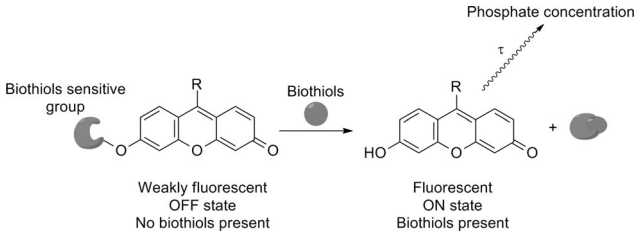

Scheme 1. Xanthenone-based fluorescent compounds and proposed functions of the simultaneous probe.

In 2005, Maeda et al. reported that 2,4-dinitrobenzenesulfonyl fluorescein derivatives can act as ON–OFF fluorescent probes toward thiols because of the highly selective aromatic nucleophilic addition of thiols to the highly electron-deficient aromatic ring.[15] These seminal studies allowed the extension of the reactive 2,4-dinitrobenzenesulfonyl derivatives to new fluorescent compounds, such as cyanine,[16] merocyanine,[17] boron-dipyrromethene (BODIPY),[18] benzothiazol,[19] and coumarin.[20] Remarkably, despite the excellent properties of xanthene-based dyes, the corresponding 2,4-dinitrobenzenesulfonyl derivatives have not been described to date. We then prepared corresponding 2,4-dinitrobenzenesulfonate derivatives of 9-[1-(2-methyl-4-methoxy-phenyl)]-6-hydroxy-3*H*-xanthen-3-one (TGII), 9-[1-(4-tert-butyl-2-methoxyphenyl)]-6-hydroxy-3*H*-xanthen-3-one (Granada Green, GG; compound **1** in the Supporting Information), and 6-hydroxy-9-isopropyl-3*H*-xanthen-3-one (*iso*-Prop-Xanth), which unfortunately presented a fast and unselective hydrolysis reaction in aqueous or methanolic solutions. Moreover, the poor solubility in pure water was also limiting for bioimaging in vivo. One possible reason for this undesirable solvolysis reaction is the low pK_a values of the starting hydroxyxanthenones, which enhances their properties as nucleofuges in a direct substitution reaction at the electron-deficient sulfur center. After obtaining these unfruitful results, we thought that the undesirable hydrolysis reaction (Scheme 2, path a) could be changed to the desired reaction if the reaction was transformed in a selective thiolysis[21] reaction (Scheme 2, path b).[22] Therefore, a new biothiol-sensitive group could be developed if the thiolysis reaction took place in aqueous solution without the interference of oxygenated nucleophiles.

In this study, we present the synthesis of the 2,4-dinitrobenzenesulfinate (DNBS) derivative of GG, that is, DNBS-GG, a new sulfinate-based[23] biothiol-sensitive group based on such a selective thiolysis reaction. This compound presents an excellent performance in terms of avoiding undesirable hydrolysis reactions, thus increasing the specificity of the fluorogenic probe toward biothiols. Moreover, DNBS-GG shows excellent behavior

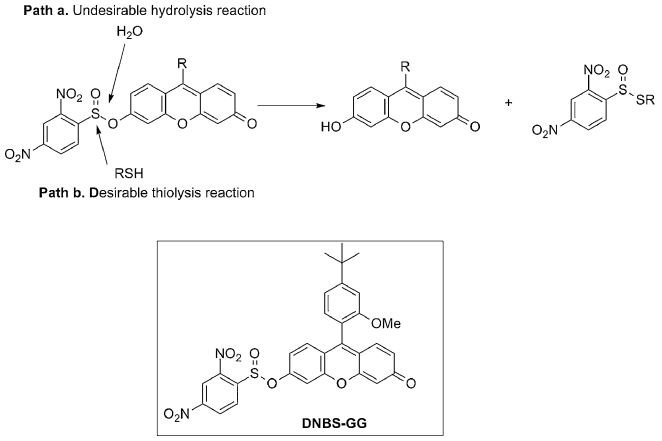

Scheme 2. Working hypothesis and structure of DNBS-GG.

as a dual probe for biothiols and phosphate anions at near-neutral pH values in vitro and in an extracellular medium.

Results and Discussion

For our purposes, the fluorescent probe should fulfill three primary conditions: 1) the nucleophilic aromatic substitution reaction should be turned off, 2) the water-promoted hydrolysis reaction should be diminished, and 3) the thiolysis reaction should be selective. To this end, less-deactivated aromatic sulfonates were prepared, but they were unreactive toward any of the previously mentioned reactions. One solution would be the use of other less-electrophilic functional groups, such as sulfinates (R^1-SO-O-R^2). In addition, the dipolar moment of the resulting molecule could increase its water solubility. The required sulfinate moiety must also be in a carefully balanced equilibrium between the undesirable hydrolysis and the desirable thiolysis reactions. Thus, the probe must be sufficiently robust to resist hydrolysis, but must also react with sulfur nucleophiles.

After some experimentation, we found that both the xanthene dye and the substitution of the sulfinate group are key factors for the success of the approach. Only the combination of GG as a xanthene dye and the 2,4-dinitro substitution of the benzene sulfinate in DNBS-GG was shown to be appropriate for this application because they are stable and soluble in water and present the expected selective reactivity toward biothiols. However, the corresponding DNBS derivatives of TGII and *iso*-Prop-Xanth were labile toward water. The reason for this different reactivity is unclear, but could be related to the higher pK_a value of GG.

The primary synthetic problem in this study is that the required 2,4-dinitrobenzenesulfinyl chloride has not been described to date.[24] Therefore, we used an unusual reaction of electron-deficient sulfonyl chlorides, which allows the reduction of the sulfur atom in situ from +6 to +4, with triethylamine as a reductant (Scheme 3).[25]

To explore the use of the new fluorescent probe to detect biologically relevant substances containing a thiol group (e.g., cysteine, homocysteine, and glutathione), the temporal de-

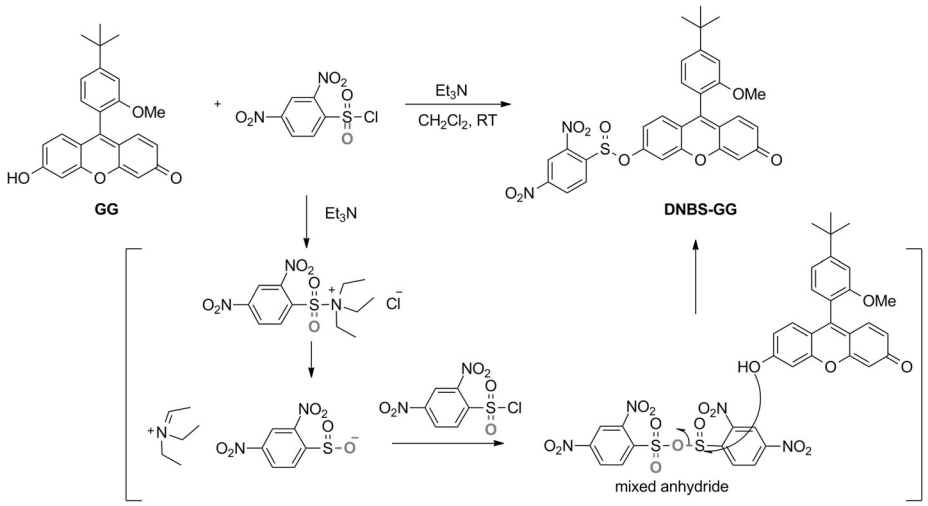

Scheme 3. Synthesis of DNBS-GG.

pendence of the DNBS-GG fluorescence emission in the presence of these biothiols was investigated at pH values of 9 (at which DNBS-GG shows the highest sensitivity to biothiols due to the influence of the pK_a value of the aliphatic thiols on the reaction), 4.80 (to check there are not undesirable hydrolysis reactions under acidic conditions, thus ruling out any potential interference of lysosomal actions in the use of the dye in cells), and 7.35 (which is interesting for physiological applications). The fluorescence emission of DNBS-GG in the absence of biothiols was very weak. However, an emission band centered at $\lambda = 520$ nm, characteristic of GG, gradually increased over time in the presence of biothiols. This fluorescence increase indicates the cleavage of DNBS-GG and its separation into two moieties, which releases the fluorescent compound GG from the electron-withdrawing 2,4-dinitrobenzene-sulfinate moiety. Figure 2A shows representative fluorescence-emission spectra at different reaction times of DNBS-GG in the presence of glutathione (GSH) at pH 7.35. Similar reactions were found upon reaction with cysteine (Cys) and homocysteine (Hcy; see Figure 2B and Figure S1 in the Supporting Information). The absorption spectra of DNBS-GG (see Figure S2 in the Supporting Information) exhibit a clear change upon reaction with thiols, which give a dual absorption band with maxima at $\lambda = 436$ and 461 nm; furthermore, the reaction gave rise to the spectral profile characteristic of free GG (absorption maximum at $\lambda =$ 495 nm).

We then attempted to analyze the fate of the DNBS-based fragment. Control experiments that used sodium propiolate as a nucleophile showed that the nucleophilic attack does not occur at the aromatic ring, as expected. The sulfur nucleophile attacks the sulfur electron-deficient center, thus initially leading to the thiolysis of DNBS-GG. After the hydrolysis of the resulting propyl 2,4-dinitrobenzenethiosulfinate[26] we could isolate 2,4-dinitrobenzenesulfinic acid.[27,28] This result is relevant because the sulfur nucleophile can be slowly regenerated over time and can influence the overall kinetics of the process.

To optimize the experimental conditions to use the DNBS-GG in biothiol detection, we further investigated the effects of the probe concentration and reaction time in the temporal generation of the fluorescent signal. First, we studied the limit in the linearity of the fluorescence signal with the concentration of the free dye (see Figures S3 and S5 in the Supporting Information). The maximum suitable concentration of the probe was selected as 6.5 μM. Biological experimental conditions were established for the reaction at 37 °C and pH 7.35 because we intended to perform the detection inside living cells. Figure 2B shows the fluorescence intensity of DNBS-GG in the presence of Cys, Hcy, or GSH at $\lambda = 519$ nm, thus increasing sharply with the reaction time from 0 to 3 h and reaching a nearly constant value at approximately 3 h. Figure S4 (see the Supporting Information) shows the relative response of DNBS-GG toward Cys, Hcy, and GSH after 2 hours of reaction under physiological experimental conditions. These results confirm a highly similar sensitivity of the probe toward the three biothiols.

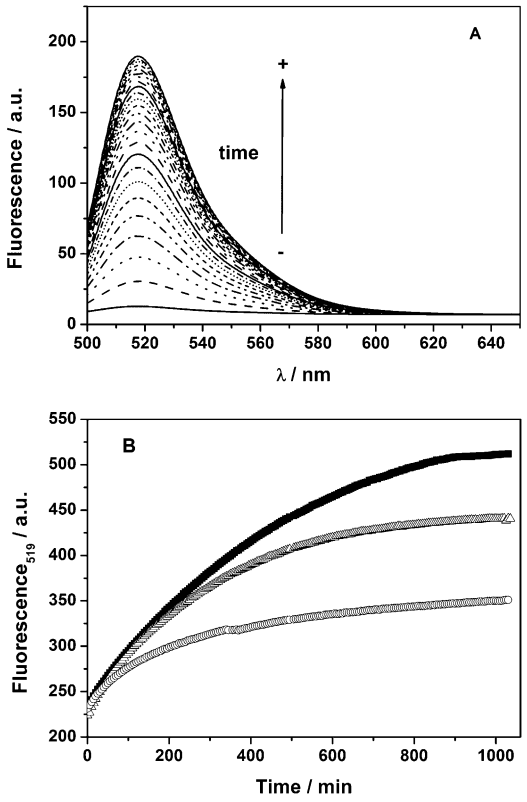

Figure 2. A) Fluorescence emission spectra ($\lambda_{ex} = 485$ nm) of DNBS-GG (6.5 μM) in the presence of 6.5 μM GSH at pH 7.35 in 10 mM Tris solution, recorded every five minutes until reaching 1300 minutes. B) Fluorescence intensity at $\lambda_{ex} = 485$ and $\lambda_{em} = 519$ nm versus time for DNBS-GG (6.5 μM) in the presence of 6.5 μM GSH (■), Cys (△), or Hcy (○) at pH 9 and 40 °C.

We also investigated potential interference from the presence of other amino acids (which lack a thiol group) or by reactive oxygen species (ROS) to study the specific response of the probe to biothiols. The increase in the fluorescence-emission intensity of DNBS-GG in the presence of L-alanine, L-serine, H_2O_2, or Fe^{II} ions was low (see Figure S4 in the Supporting Information). The low response to ROS indicates that the probe would be a good candidate for thiol detection in cases of cellular stress due to high levels of ROS in which the thiols are the first to respond to oxidative stress.

In previous studies, we have demonstrated the fluorescence-decay time of GG to be a good estimator of the phosphate-ion concentration.[14] Given that the product of the reaction between DNBS-GG and thiols is free GG, the measurements of the fluorescence-decay time must provide the basis for a dual sensor. To test the capability of the DNBS-GG dye to jointly estimate the concentrations of phosphate ions and biothiols, we studied the reaction between 6.5 μM DNBS-GG and GSH in the presence of phosphate buffer at different concentrations in the range 0–0.4 M and at pH 7.35. Experimental measurements were completed in the time-resolved regime, and Figure 3 shows the recovered results. As can be observed, the recovered lifetimes show a decrease with the phosphate-ion concentration, thus revealing that the product of the DNBS-GG cleavage is the free GG, which is sensitive toward phosphate ions through an excited-state proton-transfer (ESPT) reaction (see Scheme S1 in the Supporting Information).

The recovered fluorescence lifetimes after the reaction with the thiols are in excellent agreement with those previously reported for free GG in the presence of phosphate ions (Figure 3).[14]

The innovative dual probe for the detection of thiols and phosphate ions was also tested intracellularly by means of fluorescence-lifetime imaging microscopy (FLIM). DNBS-GG was added to the extracellular medium of human epithelioid cervix carcinoma (HeLa) cell cultures, and FLIM images were collected at different times. The evaluation of the fluorescence-intensity changes displayed with time due to biological thiols shows that the probe is cell-membrane permeable and can selectively detect thiols in living cells (Figure 4A, C). To verify this conclusion, an excess of *N*-methylmaleimide (NMM) was added to the extracellular medium to block the cellular thiols. The fluorescence signal of the probe did not appreciably change with time (Figure 4B, C). More examples of fluorescence images at different reaction times can be seen in videos in the Supporting Information.

To verify the phosphate sensitivity by the changes in the fluorescence lifetime, the cells were incubated with α-toxin, a nonspecific ionophore that opens membrane pores to allow a free flow of small ions, including the phosphate buffer added

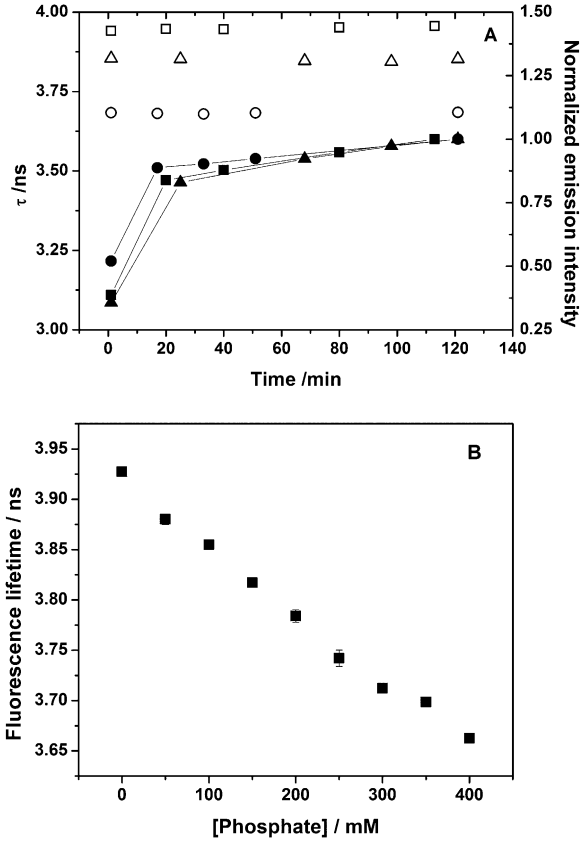

Figure 3. A) Fluorescence-decay time (open symbols, left *y* axis) and normalized emission intensity (closed symbols, right *y* axis) of DNBS-GG (6.5×10^{-6} M) in the presence of GSH (6.5×10^{-6} M) at pH 7.35 and total phosphate-ion concentration of 0 (black squares), 200 (blue triangles), and 400 mM (red circles). B) Average of the fluorescence-decay time of DNBS-GG (6.5×10^{-6} M) in the presence of GSH (6.5×10^{-6} M) at pH 7.35, collected every 10 min for 1 h of reaction in the presence of different amounts of total phosphate ions between 0 and 400 mM.

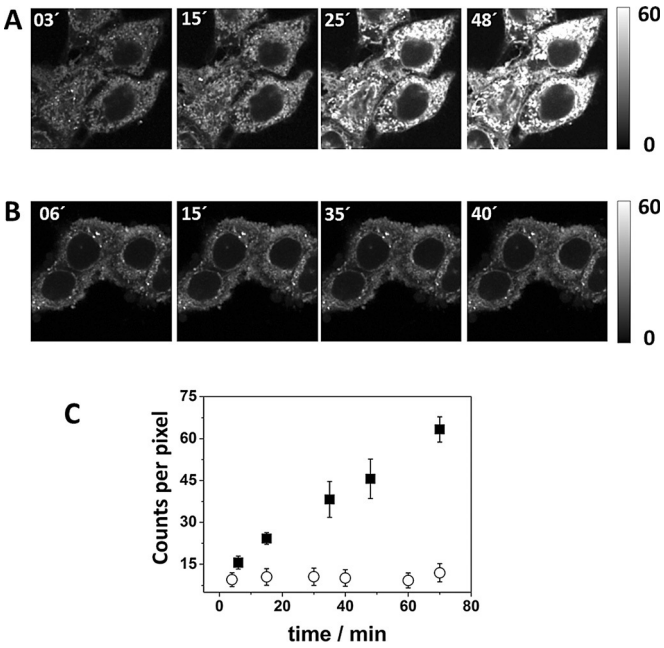

Figure 4. Fluorescence-intensity images of cell cultures with DNBS-GG (1×10^{-7} M) at different reaction times (in minutes). A) Physiological conditions with natural thiols present. B) Cells incubated with an excess of NMM. Scale bars represent 10 μm. C) Average number of photons per pixel containing the fluorescence of the probe (cell cytoplasm) from cells under physiological conditions (black squares) or incubated with an excess of NMM (open circles). Error bars represent standard deviations from the measurements of at least five different cells.

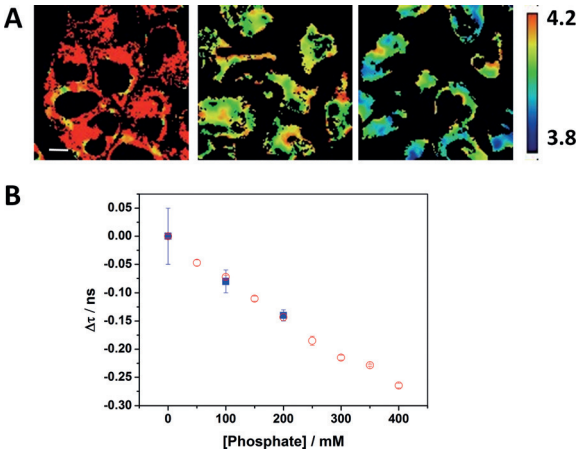

Figure 5. A) FLIM images of cells incubated with α-toxin and with DNBS-GG (1×10^{-7} M) at pH 7.35 with phosphate-ion concentrations of 0, 100, and 200 mM (arbitrary color scale). The FLIM images were collected after 30 minutes to allow the reaction of DNBS-GG with the intrinsic thiols. Scale bar represents 10 μm. B) Recovered lifetime of DNBS-GG in α-toxin-treated cells in the presence of different phosphate-ion concentrations. Error bars represent standard deviations from the measurements of at least five different images containing multiple cells.

to the extracellular media. Along with the increase in the fluorescence emission due to a reaction with the internal thiols, the FLIM images show changes in the fluorescence lifetime of the probe because of the changes in the total phosphate-ion concentration (Figure 5 A, B). Previously,[24] we have reported the kinetic rate constant of the buffer-mediated proton-transfer reaction in the ground state in different buffers by using fluorescence correlation spectroscopy (FCS) and showed that only a suitable buffer, such as phosphate, makes the reaction fast enough to compete with fluorescence emission; therefore, we could assign these changes in lifetime to phosphate ESPT among other cell species. Although $\Delta\tau$ shows a large error bar, this is intrinsic to cell-to-cell variation. Nevertheless, we have shown the excellent feasibility and specificity of this method in previous reports for following variations of the phosphate-ion concentration in living cells between 10 and 600 mM.[13;14,29]

We show that this dye can detect thiols and phosphate ions at the same time. The combined sensing of inorganic phosphate ions and GSH has a clear biological relevance. In bone tissue, the regulation of bone synthesis and degradation is modulated by oxidative stress. The molecular bases of these interactions have been proposed, and the role of specific genes that promote oxidative stress in the development of osteoporosis has been described (e.g., the *NOX4* gene promotes oxidative stress and osteoporosis,[30] whereas *FoxO1* gene expression exerts a protective effect).[31] In addition, sensing of phosphate-based energy-rich compounds and oxidative stress is relevant in biology in pathological processes that include alteration of the energetic metabolism combined with an increase in oxidative stress. Examples of these situations are cancer,[32] obesity, diabetes,[4] and hypoxia[33]. Studies that use our dye for some of these biological diseases and sensibility against phosphate compounds are in progress.

Conclusion

We have designed and synthesized a new sulfinyl xanthene derivative that can act as a simultaneous dual sensor of different analytes, such as biological biothiols and phosphate anions. The mechanism of action of this derivative implies thiolysis of the sulfinyl group of the weakly fluorescent DNBS-GG by biological biothiols, thus releasing a fluorescent GG moiety that simultaneously responds to phosphate anions through its fluorescence-decay time. The efficiency of this new dye as a dual sensor was probed in experiments at two significant pH values in vitro; that is, pH 9, at which the probe responds faster and is more sensitive to biothiols, and pH 7.35, which is required for biological applications. In both cases, we could detect the presence of cysteine, homocysteine, or glutathione and determine the phosphate-ion concentration at the same time. Note that this probe is suitable for thiol detection in cases of cellular stress due to its low response to ROS. Moreover, this new dye was tested intracellularly by using FLIM in HeLa cells and showed permeability through the cell membrane. Again, the increase in the fluorescence intensity confirmed the ability of this dye to detect thiols, and changes in the fluorescence lifetime enabled its behavior as a phosphate-ion concentration sensor.

Experimental Section

General

All reactions were performed in dry glassware in an air atmosphere. All of the commercially available reagents (2,4-dinitrobenzenesulfonyl chloride and 2,4-dinitrobenzenesulfonic acid) and solvents (triethylamine, dichloromethane, and methanol) were used without further purification. TLC analysis was performed on aluminum-backed plates coated with silica gel 60 (230–240 mesh) with F254 indicator. The spots were visualized with UV light ($\lambda=$ 254 nm) and/or staining with Ce/Mo reagent or phosphomolybdic acid solution and subsequent heating. NMR spectra were measured at room temperature and the ^{1}H NMR spectra were recorded at 500 or 600 MHz.

Synthesis and spectroscopic data of DNBS-GG

2,4-Dinitrobenzenesulfonyl chloride (29 mg, 0.11 mmol) was added to Granada Green (GG, 20 mg, 0.056 mmol) dissolved in Et_3N and CH_2Cl_2 (4 mL, 1:1 v/v; Scheme 3). The reaction was monitored by TLC analysis and 2,4-dinitrobenzenesulfonyl chloride (29 mg, 0.11 mmol) was added every 60 min until no starting material was observed. The solvent was removed by evaporation, and the residue was purified by flash chromatography with CH_2Cl_2/MeOH as the eluent to give the corresponding DNBS-GG derivative as a dark-orange solid (16 mg, 50%). ^{1}H NMR (600 MHz, [D_6]acetone): $\delta=$8.95 (d, $J=$2.7 Hz, 1H), 8.60 (dd, $J=$9.2, 2.8 Hz, 1H), 7.66 (d, $J=$9.2 Hz, 1H), 7.35 (s, 1H), 7.34 (d, $J=$2.4 Hz, 1H), 7.29–7.25 (m, 3H), 7.17 (dd, $J=$8.8, 2.4 Hz, 1H), 7.08 (d, $J=$9.8 Hz, 1H), 6.44 (dd, $J=$9.8, 1.7 Hz, 1H), 6.16 (d, $J=$1.7 Hz, 1H), 3.82 (s, 3H), 1.44 ppm (s, 9H); ^{13}C NMR (151 MHz, [D_6]acetone): $\delta=$187.1 (C), 161.1 (C), 160.9 (C), 159.5 (C), 157.9 (C), 156.2 (C), 148.1 (C), 146.1 (C), 143.7 (C), 133.7 (CH), 133.2 (CH), 133.0 (CH), 132.8 (CH), 132.1 (CH), 130.2 (C), 124.8 (CH), 124.6 (CH), 123.2 (C), 121.0 (C), 120.9 (C), 120.5 (CH), 118.3 (CH), 111.7 (CH), 109.4 (CH), 107.9 (CH), 57.8 (CH_3), 37.7 (C),

33.3 (CH_3); LSIMS (FAB): *m/z* calcd for $C_{30}H_{24}N_2O_9S$: 588.12 [M^+]; found: 588.12.

Preparation of solutions

Tris(hydroxymethyl)aminomethane (Tris) buffer solutions were prepared by mixing the required amounts of Trizma base and Tris–HCl (both from Sigma-Aldrich) to obtain the desired pH value. For the preparation of phosphate buffer (pH 6.8) solutions, $NaH_2PO_4{\cdot}H_2O$ and $Na_2HPO_4{\cdot}7H_2O$ (both from Fluka, puriss. p.a.) were used. All of the solutions were prepared with Milli-Q water as the solvent. All of the chemicals were used as received without further purification. A stock solution of DNBS-GG (10^{-4} M) in ethanol was prepared. From this stock solution, aqueous solutions with a final concentration of 1×10^{-5} M of dye and pH 7.35 in Tris buffer were prepared. The required amounts of this solution and thiol stock solution were added to obtain the desired concentrations of DNBS-GG and thiol in Tris buffer (20 mm) at pH 7.35.

Solutions of all of the compounds for time-resolved fluorescence measurements were prepared so that the absorbance of the final solutions at λ_{ex} was lower than 0.1. Solutions were kept cool in the dark when not in use to avoid possible deterioration by exposure to light and heat. The solutions were not degassed.

Instrumentation

Absorption spectra were recorded on a Perkin–Elmer Lambda 650 UV/Vis spectrophotometer with a temperature-controlled cell. Steady-state fluorescence emission spectra were performed on a JASCO FP-6500 spectrofluorometer equipped with a 450 W xenon lamp for excitation and an ETC-273T temperature controller at 20 °C. The pH values of the solutions were measured immediately before the fluorescence measurements at the same temperature.

Fluorescence-decay traces of solutions were recorded by the single-photon timing method on a FluoTime 200 fluorometer (PicoQuant, Inc.). The excitation was achieved with a LDH-485 laser head (PicoQuant, Inc.), and the observation was performed through a monochromator at $\lambda = 515$ nm. The pulse repetition rate was 20 MHz. Fluorescence-decay histograms were collected in 1320 channels using cuvettes of 10×10 mm. The time increment per channel was 36 ps. Histograms of the instrument-response functions (using a LUDOX scatterer) and sample decays were recorded until they typically reached 2×10^4 counts in the peak channel. Three fluorescence decays were recorded for all of the samples. The fluorescence-decay traces were individually analyzed by using an iterative deconvolution method with exponential models that employed FluoFit software (PicoQuant).

Fluorescence-lifetime images were recorded on a MicroTime 200 fluorescence-lifetime microscope system (PicoQuant, Inc.) and the time-tagged time-resolved (TTTR) methodology, which permits fluorescence-decay histograms to be reconstructed from molecules in the confocal volume. The excitation source consisted of a laser diode head (LDH) pulsed laser at $\lambda = 470$ nm (PicoQuant) that operates at a repetition rate of 20 MHz. The light beam was directed onto a dichroic mirror (500DCXR) to the oil-immersion objective (numerical aperture = 1.4, 100×) of an inverted microscope system IX-71 (Olympus). The collected fluorescence light was filtered by an HP500LP long-pass filter (AHF/Chroma) and focused onto a confocal aperture of 75 μm. After the aperture, the transmitted light was refocused onto a single-photon avalanche diode SPCM-AQR 14 (Perkin–Elmer) after the signal passed through a 520/35 filter (Chroma). The data acquisition was performed with a TimeHarp 200 TCSPT module (PicoQuant, Inc.) in the TTTR mode, which enabled the reconstruction of the lifetime histogram. Raw images were recorded by raster scanning of an area of 80×80 μm, with a resolution of 512×512 pixels. The photons of each pixel were temporally sorted with respect to the excitation pulse in the histograms with a time resolution of 29 ps channel^{-1}.

Cell culture

The human epithelioid cervix carcinoma (HeLa; ATCC No. CCL-2) cell line was provided by the Cell Culture Facility, University of Granada. The HeLa cells were grown in the Dulbecco modified Eagle medium (DMEM) supplemented with 10% (v/v) fetal bovine serum (FBS), 2 mm glutamine, 100 U mL^{-1} penicillin, and 0.1 μg mL^{-1} streptomycin in a humidified 5% CO_2 incubator.

For the FLIM microscopy experiments, the HeLa cells were seeded onto coverslips (25 mm) in six-well plates at a density of 11 250 cells cm^{-2}. On the day of the experiment, the cells were washed twice with Krebs–Ringer phosphate medium (118 mm NaCl, 5 mm KCl, 1.2 mm $MgSO_4$, 1.3 mm $CaCl_2$, 1.2 mm KH_2PO_4, 30 mm 4-(2-hydroxyethyl)-1-piperazineethanesulfonic acid (HEPES), pH 7.4) and incubated in the same medium with effectors. When *N*-methylmaleimide (NMM) was used to block the intracellular thiols, the cells were preincubated with 1 mm NMM for 20 min. NMM was maintained in the medium during the FLIM experiments.

Cell permeabilization

Cells were permeabilized as reported.[14] Briefly, HeLa cells were seeded onto coverslips in 12-well plates. On the day of the experiment, the cells were washed twice with phosphate-buffered saline (PBS) and were perforated by incubation for 15 min at 37 °C with 2 μg mL^{-1} α-toxin in permeabilization buffer (20 mm potassium 3-(*N*-morpholino)propanesulfonate (pH 7.0), 250 mm mannitol, 1 mm potassium adenosine triphosphate (ATP), 3 mm $MgCl_2$, and 5 mm potassium glutathione). Subsequently, the cells were washed twice with PBS and were analyzed by using FLIM in the presence of different concentrations of phosphate ions in the assay medium.

Acknowledgements

This research was funded by MINECO (project CTQ2014-53598) and CEI-BioTic (UGR).

Keywords: anions · fluorescence lifetime imaging microscopy · fluorescent probes · intracellular imaging agents · thiols

[1] a) C. Ding, A. Zhu, Y. Tian, *Acc. Chem. Res.* **2014**, *47*, 20; b) P. D. Howes, R. Chandrawati, M. M. Stevens, *Science* **2014**, *346*, 1247390.
[2] X. Chen, Y. Zhou, X. Peng, J. Yoon, *Chem. Soc. Rev.* **2010**, *39*, 2120.
[3] a) N. Majed, Y. Li, A. Z. Gu, *Current Opinion in Biotechnology* **2012**, *23*, 852; b) S. Khoshniat, A. Bourgine, M. Julien, P. Weiss, J. Guicheux, L. Beck, *Cell. Mol. Life Sci.* **2011**, *68*, 205; c) C. Bergwitz, H. Jüppner, *Adv. chronic kidney disease* **2011**, *18*, 132.
[4] T. Yokota, S. Kinugawa, M. Yamato, K. Hirabayashi, T. Suga, S. Takada, K. Harada, N. Morita, N. Oyama-Manabe, Y. Kikuchi, K. Okita, H. Tsutsui, *Diabetes Care* **2013**, *36*, 1341.
[5] Y. Urano, M. Kamiya, K. Kanda, T. Ueno, K. Hirose, T. Nagano, *J. Am. Chem. Soc.* **2005**, *127*, 4888.
[6] A. Martínez-Peragón, D. Miguel, R. Jurado, J. Justicia, J. M. Alvarez-Pez, J. M. Cuerva, L. Crovetto, *Chem. Eur. J.* **2014**, *20*, 447.
[7] M. Kamiya, D. Asanuma, E. Kuranaga, A. Takeishi, M. Sakabe, M. Miura, T. Nagano, Y. Urano, *J. Am. Chem. Soc.* **2011**, *133*, 12960.

[8] D. Srikun, A. E. Albers, C. I. Nam, A. T. Iavarone, C. J. Chang, *J. Am. Chem. Soc.* **2010**, *132*, 4455.
[9] M. Kawaguchi, T. Okabe, S. Okudaira, K. Hanaoka, Y. Fujikawa, T. Terai, T. Komatsu, H. Kojima, J. Aoki, T. Nagano, *J. Am. Chem. Soc.* **2011**, *133*, 12021.
[10] T. Terai, R. Tomiyasu, T. Ota, T. Ueno, T. Komatsu, K. Hanaoka, Y. Urano, T. Nagano, *Chem. Commun.* **2013**, *49*, 3101.
[11] Y. Cheng, H. Xie, P. Sule, H. Hassounah, E. A. Graviss, Y. Kong, J. D. Cirillo, J. Rao, *Angew. Chem. Int. Ed.* **2014**, *53*, 9360; *Angew. Chem.* **2014**, *126*, 9514.
[12] M. Kamiya, Y. Urano, N. Ebata, M. Yamamoto, J. Kosuge, T. Nagano, *Angew. Chem. Int. Ed.* **2005**, *44*, 5439; *Angew. Chem.* **2005**, *117*, 5575.
[13] J. M. Paredes, M. D. Giron, M. J. Ruedas-Rama, A. Orte, L. Crovetto, E. M. Talavera, R. Salto, J. M. Alvarez-Pez, *J. Phys. Chem. B* **2013**, *117*, 8143.
[14] A. Martínez-Peragón, D. Miguel, A. Orte, A. J. Mota, M. J. Ruedas-Rama, J. Justicia, J. M. Alvarez-Pez, J. M. Cuerva, L. Crovetto, *Org. Biomol. Chem.* **2014**, *12*, 6432.
[15] a) H. Maeda, H. Matsuno, M. Ushida, K. Katayama, K. Saeki, N. Itoh, *Angew. Chem. Int. Ed.* **2005**, *44*, 2922; *Angew. Chem.* **2005**, *117*, 2982; b) H. Maeda, K. Yamamoto, I. Kohno, L. Hafsi, N. Itoh, S. Nakagawa, N. Kanagawa, K. Suzuki, T. Uno, *Chem. Eur. J.* **2007**, *13*, 1946.
[16] D. Maity, T. Govindaraju, *Org. Biomol. Chem.* **2013**, *11*, 2098.
[17] S.-P. Wang, W.-J. Deng, D. Sun, M. Yan, H. Zheng, J.-G. Xu, *Org. Biomol. Chem.* **2009**, *7*, 4017.
[18] X. Li, S. Qian, Q. He, B. Yang, J. Li, Y. Hu, *Org. Biomol. Chem.* **2010**, *8*, 3627.
[19] W. Sun, W. Li, J. Li, J. Zhang, L. Du, M. Li, *Tetrahedron Lett.* **2012**, *53*, 2332.
[20] a) J. Li, C.-F. Zhang, Z.-Z. Ming, W.-C. Yang, G.-F. Yang, *RSC Adv.* **2013**, *3*, 26059; see also: b) J. Bouffard, Y. Kim, T. M. Swager, R. Weissleder, S. A. Hilderbrand, *Org. Lett.* **2008**, *10*, 37; c) M. Li, H. Ge, R. L. Arrowsmith, V. Mirabello, S. W. Botchway, W. Zhu, S. I. Pascu, T. D. James, *Chem. Commun.* **2014**, *50*, 11806.
[21] It is known that sulfonate esters can be *trans*-thioesterificated by thiols at high temperatures, see: a) A. K. Chakraborti, M. K. Nayak, L. Sharma, *The Journal of Organic Chemistry* **1999**, *64*, 8027; b) T. Okuyama, H. Takano, K. Senda, *Bull. Chem. Soc. Japan* **1996**, *69*, 2639; c) T. Okuyama, *Bull. Chem. Soc. Japan* **1996**, *69*, 3281.
[22] A selective hydrolysis reaction is also the basis of the analysis of superoxide ions, see: H. Maeda, K. Yamamoto, Y. Nomura, I. Kohno, L. Hafsi, N. Ueda, S. Yoshida, M. Fukuda, Y. Fukuyasu, Y. Yamauchi, N. Itoh, *J. Am. Chem. Soc.* **2005**, *127*, 68.
[23] A related approach based on *tert*-butylsulfinate thiolysis has been recently reported, although the direct application to our case was unsuccessful owing to the lability of the final product toward unselective hydrolysis in aqueous and methanolic solutions; see: S. R. Malwal, A. Labade, A. S. Andhalkar, K. Sengupta, H. Chakrapani, *Chem. Commun.* **2014**, *50*, 11533.
[24] Even the corresponding 2,4-dinitrobenzenesulfinyl acid has not been described to date by using known protocols, see: C. Lee, L. Field, *Synthesis* **1990**, *1990*, 391.
[25] T. Netscher, P. Bohrer, *Tetrahedron Lett.* **1996**, *37*, 8359.
[26] a) T. Takata, Y. H. Kim, S. Oae, *Bull. Chem. Soc. Japan* **1981**, *54*, 1443; b) S. Oae, T. Takata, *Tetrahedron Lett.* **1980**, *21*, 3213.
[27] S. Detoni, D. Hadzi, *J. Chem. Soc.* **1955**, 3163.
[28] a) C. S. Baker, H. A. Strobel, *J. Phys. Chem.* **1979**, *83*, 728; b) H. Koshima, H. Miyamoto, I. Yagi, K. Uosaki, *Molecul. Cryst. Liquid Crystals* **2004**, *420*, 79.
[29] J. M. Paredes, A. Orte, L. Crovetto, J. M. Alvarez-Pez, M. J. Ruedas-Rama, E. M. Talavera, *Phys. Chem. Chem. Phys.* **2010**, *12*, 323.
[30] C. Goettsch, A. Babelova, O. Trummer, R. G. Erben, M. Rauner, S. Rammelt, N. Weissmann, V. Weinberger, S. Benkhoff, M. Kampschulte, B. Obermayer-Pietsch, L. C. Hofbauer, R. P. Brandes, K. Schröder, *J. Clin. Invest.* **2013**, *123*, 4731.
[31] M.-T. Rached, A. Kode, L. Xu, Y. Yoshikawa, J.-H. Paik, R. A. DePinho, S. Kousteni, *Cell Metab.* **2010**, *11*, 147.
[32] J. A. Hess, M. K. Khasawneh, *BBA Clin.* **2015**, *3*, 152.
[33] A. Almeida, M. Delgado-Esteban, J. P. Bolaños, J. M. Medina, *J. Neurochem.* **2002**, *81*, 207.

Received: July 16, 2015
Published online on September 16, 2015